Mechanisms of Action of Mixed Solid−Liquid Antifoams. 2. Stability of Oil Bridges in Foam Films

Nikolai D. Denkov*

Usine Silicones, RHODIA Chimie, CRIT C, 55 Rue des Freres Perret BP 22, 69191 Saint Fons Cedex, France

Received February 23, 1999. In Final Form: May 6, 1999

In the first part of this study we described the process of destabilization of foam films by mixed (silica−silicone oil) antifoam drops as observed with a high-speed video camera. The drops formed oil bridges, which stretched with time and eventually ruptured the foam films. Remarkably, two types of bridges could be distinguished: (i) mechanically unstable ones, which stretched and ruptured the films within several milliseconds, and (ii) metastable ones, that existed for a much longer period (up to several seconds). The stability of oil bridges is theoretically analyzed in the current article, which presents a further development of the model by Garrett (*J. Colloid Interface Sci.* **1980**, *76*, 587). The deformation of the foam film surfaces, which was previously neglected, is explicitly taken into account. The effect of several governing factors (three-phase contact angles, film thickness, size of the bridge, presence of spread oil layer) on the evolution and stability of the oil bridges is analyzed. The calculations show that the bridge stability depends primarily on two factors: (i) the contact angle oil−water−air and (ii) the relative size of the bridge (with respect to the film thickness). Mechanically stable bridges can be formed at any value of the three-phase contact angle if the relative size of the bridge is below a given critical value. Above the critical size, the bridge stability is determined by the contact angle (i.e., by the corresponding bridging coefficient *B*, as introduced by Garrett). The reduced stability of the bridges in the presence of a prespread oil layer is explained by an accumulation of oil in the bridge (from the spread layer), which leads to an actual increase of the size of the bridge. The theoretical predictions are compared with the experimental results and are discussed from the viewpoint of the mechanisms of antifoam action.

Introduction

In the first part of this study[1] we applied several complementary experimental methods to reveal what is the actual mechanism of foam destruction by mixed (silica−silicone oil) antifoams in solutions of sodium dioctyl sulfosuccinate (AOT). The results showed that the antifoam particles (emulsified drops or lenses floating on the solution surface) made unstable bridges in the foam films. The bridges stretched with time due to uncompensated capillary pressures across the oil−water and oil−air interfaces (see below for details) and eventually became perforated and ruptured, resulting in subsequent destruction of the entire foam film (see Figure 11 in ref 1). For brevity, hereafter we denote this mechanism of film destruction as the "bridging−stretching" mechanism.

Two particular and somewhat unexpected features of the bridging−stretching mechanism emerged from the observations on our experimental system. First, we could distinguish two types of bridges: (i) inherently unstable bridges, which rapidly stretched and ruptured the film within several milliseconds, and (ii) metastable bridges, which survived for a much longer period (from a fraction of a second up to several seconds), during which a slow change in the bridge shape was observed, followed by a sudden and ultrarapid bridge expansion and film rupture. We interpret the latter process as a transition of the bridges from a mechanically *metastable* configuration to an *unstable* one (more precise definitions of these terms are given below). Second, we observed a strong dependence of the bridge stability on the presence of a prespread oil layer located on the surfaces of the foam film. In the absence of prespread silicone oil, the entry of an antifoam particle (most probably containing both oil and silica) typically lead to spreading of oil from the particle without film rupture; that is, the formed oil bridges were relatively stable. On the contrary, in the presence of a spread oil layer (even as thin as several nanometers) the formed oil bridges were either metastable or inherently unstable. Qualitatively, the bridge stability decreased with the amount of spread oil on the film surface.

The stability of oil bridges in foam films was theoretically studied by Garrett.[2,3] He analyzed whether a liquid bridge obeying the Neumann's triangle (three-phase contact angles satisfying the vectorial balance of the interfacial tensions at the contact line) could be in mechanical equilibrium, viz. whether the capillary pressure jumps across the interfaces can be balanced—see Figure 1. The analysis showed that if the contact angle oil−water−air $\alpha_W > \pi/2$ (or the angle $\theta_{OW} \equiv \pi - \alpha_W < \pi/2$, in Garrett's notation), then the capillary pressure jump across the oil−water interface $\Delta P_{OW} \equiv P_O - P_W$, is always smaller than the pressure jump across the oil−air interface $\Delta P_{OA} \equiv P_O - P_A$. In other words, it is impossible to satisfy simultaneously the Neumann triangle and the capillary pressure balance, which are both necessary conditions for mechanical equilibrium of the system. One important feature of Garrett's model is that the surfaces of the foam film are assumed to be perfectly planar. As a result of this approximation, the capillary pressure jump across the air−water interface $\Delta P_{AW} \equiv P_A - P_W$ is by definition equal to zero in this model. In conclusion, the bridges with $\alpha_W > \pi/2$ are considered mechanically unstable in Garrett's

* To whom correspondence should be addressed. Permanent address: Laboratory of Thermodynamics and Physicochemical Hydrodynamics, Faculty of Chemistry, Sofia University, 1 James Bourchier Ave., 1126 Sofia, Bulgaria. Phone: (+359) 2-962 5310. Fax: (+359) 2-962 5643. E-mail: ND@LTPH.BOL.BG.

(1) Denkov, N. D.; Cooper, P.; Martin, J.-Y. *Langmuir* **1999**, *15*, 8514.

(2) Garrett, P. R. *J. Colloid Interface Sci.* **1980**, *76*, 587.

(3) Garrett, P. R. In *Defoaming: Theory and Industrial Applications*; Garrett, P. R., Ed.; Marcel Dekker: New York, 1993; Chapter 1.

10.1021/la990214y CCC: $18.00
Published on Web 11/23/1999

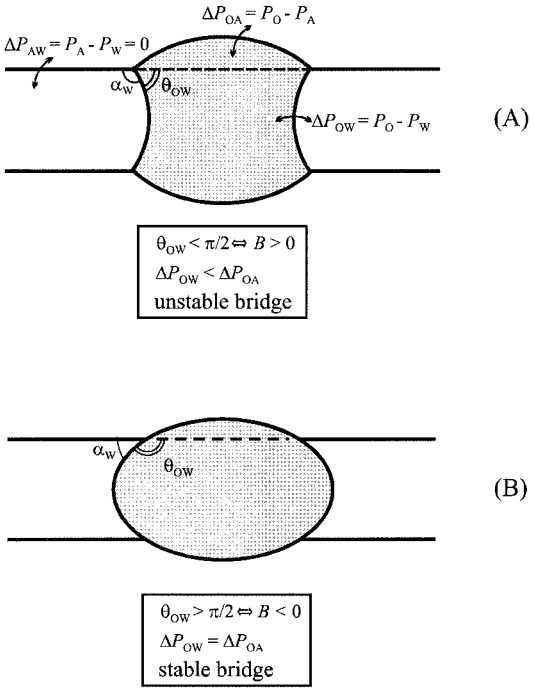

Figure 1. Schematic presentation of an oil bridge in a planar foam film:[2,3] (A) unstable bridge of positive bridging coefficient, $B > 0$ ($\theta_{OW} < 90°$; $\alpha_W > 90°$); (B) stable bridge of negative bridging coefficient, $B < 0$ ($\theta_{OW} > 90°$; $\alpha_W < 90°$).

model, while at $\alpha_W < \pi/2$ (which is equivalent to $\theta_{OW} > \pi/2$ in Garrett's notation) one can construct a liquid bridge of a certain size that satisfies simultaneously both conditions for mechanical equilibrium, namely, the Neumann triangle and the capillary pressure balance.

As shown by Garrett,[3] the geometrical requirement $\theta_{OW} < \pi/2$ is equivalent to the following relationship between the interfacial tensions

$$B \equiv \sigma_{AW}^2 + \sigma_{OW}^2 - \sigma_{OA}^2 > 0 \qquad (1)$$

where the subscripts AW, OW, and OA denote the air−water, oil−water, and oil−air interfaces, respectively. B in eq 1 is the so-called "bridging coefficient", which was introduced by Garrett as a quantitative criterion for bridge stability. Positive values of B correspond to $\theta_{OW} < \pi/2$ ($\alpha_W > \pi/2$) and unstable bridges, while negative values of B correspond to $\theta_{OW} > \pi/2$ ($\alpha_W < \pi/2$) and mechanically stable bridges.

The actual mechanism by which the oil bridges rupture the foam films was not specified in detail in the original paper.[2] Garrett suggested[2] that the disbalance of pressures at positive B "would presumably give rise to enhanced drainage [of aqueous surfactant solution] away from the droplet". On the contrary, at negative B "the unbalanced force acts in a direction opposing film drainage". Probably these comments have lead most of the researchers in this area to consider the film destabilization by oil bridges in terms of the bridging−dewetting mechanism (see Figure 1 in ref 1), similar to the process of dewetting of solid particles in foam films as observed by Dippenaar[4] and theoretically modeled by Frye and Berg.[5]

In a later study Garrett[3] pointed out another possible mechanism of film rupture. As $\alpha_W \to \pi$ (which is equivalent to $\alpha_O \to 0$, with α_O being the three-phase contact angle water−oil−air)," the curvature of the oil-air interfaces

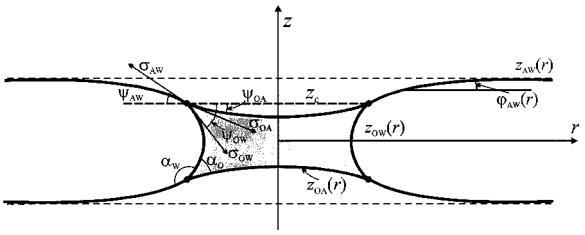

Figure 2. Schematic presentation of an oil bridge in a foam film with deformable surfaces. The foam film surfaces far away from the bridge are planar.

will of necessity become concave ... [and] the point of rupture could be at the center of the expanding oil lens as the two concave air−oil surfaces approach one another"[3]—see Figure 2. It is important to note that the contact angle α_O in our experimental system[1] was indeed very small. The idea of film rupture at the center of an oil bridge can be traced back to an article by Ross,[6] who wrote: "The total effect [of bridging] is the replacement in the film of a liquid capable of sustaining stable films by a liquid which does not possess that property. The film is thinnest precisely at the place where it is composed *entirely* of the antifoaming agent and it is therefore at this spot that rupture of the film can be expected to take place." However, Ross[6] imposed a very strong condition for realization of this mechanism, namely, that the spreading coefficient S should be positive, while later studies[3,7] showed that this is not a necessary condition for antifoaming action. In fact, this picture (biconcave oil bridge which ruptures in the center) is what we observed in our experiments and what we call the bridging−stretching mechanism.[1]

The aim of the current study is to analyze theoretically in more detail the stability of foam films in the presence of oil bridges. First, we often observed a notable deformation of the two film surfaces upon the formation of the bridge (in particular, when metastable bridges appeared). As mentioned above, in Garrett's model[2] the film surfaces were assumed to be perfectly flat and it was not clear in advance whether the observed surface deformation could change significantly the predictions of the theoretical model. As we show below, the deformability of the film surfaces turned out to be an important effect, and some new features of the bridge stability have emerged from the more detailed consideration. Second, the actual mechanism of bridge stretching due to the disbalance of capillary pressures had not been entirely clear, and we have clarified further this point. Third, we have been able to explain the observed effect of the prespread oil layer, as well as the presence of metastable bridges and their transition to an unstable configuration. In this way we have achieved two goals: (i) the main experimental observations have been explained, and (ii) the understanding of the film stability in the presence of oil bridges is further enhanced.

Physical and Mathematical Background

In this section we outline the basic equations describing the shape of fluid interfaces in mechanical equilibrium. The particular model of oil bridges in foam films, which is adopted in our consideration, is described afterward.

Laplace Equation of Capillarity. The shape of the interfaces in mechanical equilibrium must obey the Laplace equation of capillarity, which relates the capillary

(4) Dippenaar, A. *Int. J. Miner. Process.* **1982**, *9*, 1.
(5) Frye, G. C.; Berg, J. C. *J. Colloid Interface Sci.* **1989**, *127*, 222.
(6) Ross, S. *J. Phys. Colloid Chem.* **1950**, *54*, 429.
(7) Garrett, P. R.; Davis, J.; Rendall, H. M. *Colloids Surf., A: Physicochem. Eng. Aspects* **1994**, *85*, 159.

pressure jump across the interface ΔP with the curvature of the interface

$$\Delta P = \sigma(1/R_1 + 1/R_2) \tag{2}$$

Here σ is the interfacial tension, while R_1 and R_2 are the two principle radii of curvature. Note that in general the two radii of curvature could be negative or positive or have different signs for a given interface. In our system we can neglect the effect of gravity (an estimate of the gravity term is presented below) and can consider the bridge as being symmetrical with respect to (i) a plane parallel to the nonperturbed foam film surfaces and (ii) an axis perpendicular to the plane of the film and passing through the center of the bridge—see Figure 2. In this case the Laplace equation of capillarity can be expressed as a system of two ordinary differential equations of first order[8,9]

$$\frac{\mathrm{d}\sin\varphi}{\mathrm{d}r} + \frac{\sin\varphi}{r} = \frac{\Delta P}{\sigma} \tag{3}$$

$$\frac{\mathrm{d}z}{\mathrm{d}r} = \tan\varphi \tag{4}$$

with two unknown functions, $z(r)$ and $\varphi(r)$, which describe the coordinates of the points at the interface and the running slope angle, respectively (see Figure 2). Here the z axis is chosen to coincide with the axis of symmetry ($-\infty < z < +\infty$) and r is a polar coordinate ($0 \le r < \infty$). Since the bridge is symmetrical with respect to the plane $z = 0$, one can consider only the upper half of the system ($z \ge 0$).

Neumann Vectorial Triangle. The mechanical equilibrium of a heterogeneous system requires also a balance of the surface tensions acting on the three-phase contact lines. For fluid phases this requirement is represented by the so-called Neumann vectorial triangle

$$\boldsymbol{\sigma}_{\mathrm{AW}} + \boldsymbol{\sigma}_{\mathrm{OW}} + \boldsymbol{\sigma}_{\mathrm{OA}} = 0 \tag{5}$$

The vectors $\boldsymbol{\sigma}_{\mathrm{AW}}$, $\boldsymbol{\sigma}_{\mathrm{OW}}$, and $\boldsymbol{\sigma}_{\mathrm{OA}}$ have magnitudes equal to the respective scalar interfacial tensions. The vectors are oriented in such a way that they are simultaneously tangential to the respective interface and perpendicular to the three-phase contact line (Figure 2). The vectorial eq 5 can be presented as a set of two independent trigonometric equations connecting the scalar interfacial tensions with the slope angles, ψ_{OA}, ψ_{AW}, and ψ_{OA} at the contact line

$$\sigma_{\mathrm{AW}}\cos\psi_{\mathrm{AW}} = \sigma_{\mathrm{OW}}\cos\psi_{\mathrm{OW}} + \sigma_{\mathrm{OA}}\cos\psi_{\mathrm{OA}} \tag{6}$$

$$\sigma_{\mathrm{AW}}\sin\psi_{\mathrm{AW}} = \sigma_{\mathrm{OW}}\sin\psi_{\mathrm{OW}} + \sigma_{\mathrm{OA}}\sin\psi_{\mathrm{OA}} \tag{7}$$

From a mathematical viewpoint, eqs 6 and 7 appear as boundary conditions for solving the Laplace equation of capillarity (eqs 3 and 4).

Particular Solutions of the Laplace Equation. The particular function describing the profile of an interface can be found as a solution of the Laplace equation of capillarity, and it depends on both the boundary conditions and the value of the capillary pressure ΔP. A detailed analysis of the possible solutions can be found in ref 8−11. In general, the interface could be planar ($\Delta P = 0$; $1/R_1 = 1/R_2 = 0$), spherical ($1/R_1 = 1/R_2 \neq 0$), or cylindrical ($1/R_1 = 0$, $1/R_2 \neq 0$) or the surface generatrix could be part of a catenoid ($\Delta P = 0$, $1/R_1 = -1/R_2 \neq 0$), a nodoid, or an unduloid. Explicit expressions for these functions are presented in the following section, where we discuss the shapes of the different interfaces in our system.

Model of the Liquid Bridge

The central question in the present analysis is whether a liquid bridge formed in a foam film can be mechanically stable. Following the idea of Garrett,[2,3] we try to construct a bridge which satisfies simultaneously the Laplace equation of capillarity and the Neumann triangle. If these two conditions can be satisfied at given values of the interfacial tensions, the film thickness, and the volume of the bridge, then the bridge is considered as being in mechanical equilibrium. In a second stage of the analysis, which is presented in the next section, we investigate whether the obtained configuration corresponds to a stable or unstable equilibrium.

The main difference of the present theoretical model from the previous model[2] is that the foam film surfaces are considered as deformable. This makes the model much more complex because a variety of solutions of the Laplace equation of capillarity are in principle possible. One should carefully screen all of the possible solutions to check which of them can be realized at given prescribed conditions (bridge volume, foam film thickness, three-phase contact angles, etc.). Below we first analyze which of the solutions could be used for description of the different interfaces (OA, AW, and OW); afterward the algorithm used to "build-up" a bridge satisfying the Laplace equation of capillarity at the respective conditions is explained.

Oil−Air Interface. When an interface meets the axis of revolution, as it is the case with the oil−air interface in our system, then it must be a part of a sphere (see Figure 3)

$$z_{\mathrm{OA}}(r) = z_{0\mathrm{S}} + \mathrm{sgn}(\Delta P_{\mathrm{OA}})\sqrt{R_{\mathrm{OA}}^2 - r^2} \qquad (0 \le r \le r_{\mathrm{C}}) \tag{8}$$

$$\tan\varphi_{\mathrm{OA}} = -\mathrm{sgn}(\Delta P_{\mathrm{OA}})\frac{r}{\sqrt{R_{\mathrm{OA}}^2 - r^2}} \qquad (0 \le r \le r_{\mathrm{C}}) \tag{9}$$

$$R_{\mathrm{OA}} = 2\sigma_{\mathrm{OW}}/\Delta P_{\mathrm{OA}} \tag{10}$$

The function $\mathrm{sgn}(x)$ is equal to $+1$ or -1 for positive or negative values, respectively, of its argument. If the capillary pressure jump $\Delta P_{\mathrm{OA}} \equiv P_{\mathrm{O}} - P_{\mathrm{A}}$ is positive, then the cap of the oil bridge is convex (see Figure 3A). On the contrary, if ΔP_{OA} is negative, then the cap of the oil bridge is concave (Figure 3B). The vertical displacement of the spherical surface (viz. the coordinate of the geometrical center of the spherical surface $z_{0\mathrm{S}}$) depends on the boundary conditions at the three-phase contact line: the slope angle ψ_{OA} and the height of the contact line z_{C}.

Air−Water Interface. The experiments[1] in the Scheludko cell showed that the oil bridge perturbs the film surfaces by diminishing the local film thickness by between 100 and 500 nm. The radius of the perturbed spot was

(8) Princen, H. M. In *Surface and Colloid Science*; Matijevic, E., Ed.; Wiley: New York, 1969; Vol. 2, Chapter 1.
(9) Kralchevsky, P. A.; Danov, K. D.; Denkov, N. D. In *Handbook of Surface and Colloid Chemistry*; Birdi, K. S., Ed.; CRC Press: New York, 1997; Chapter 11.
(10) Abramowitz, M.; Stegun, I. A. *Handbook of Mathematical Functions*; Dover: New York, 1965.
(11) Finn, R. *Equilibrium Capillary Surfaces*; Springer-Verlag: New York, 1986.

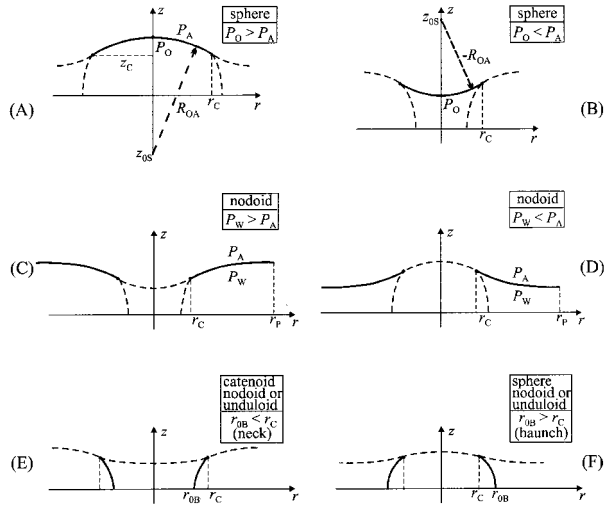

Figure 3. Different possible shapes of the oil-air (A and B), air−water (C and D), and oil−water (E and F) interfaces.

typically 10−50 μm, while the rest of the foam film thinned down without being notably affected by the presence of the bridge (until eventually the bridge stretched and ruptured the film). These observations suggest that it is reasonable to model the air−water interface in the perturbed zone as part of a surface obeying the Laplace equation of capillarity and having a horizontal tangent, $dz_{AW}/dr = 0$, at the periphery of the perturbed zone, $r_P > 0$. From all possible solutions of the Laplace equation, only a planar surface and a curved surface, generated by revolving a nodoid around the axis of symmetry, satisfy these requirements—the cylinder, the unduloid, and the catenoid have no horizontal tangent at any value of r, while the sphere has a horizontal tangent only at $r = 0$. Therefore, the air−water interface can be represented only as a plane (when $\Delta P_{AW} = 0$) or as a curved interface generated by a nodoid ($\Delta P_{AW} \neq 0$). In the latter case two possibilities have to be distinguished: if $\Delta P_{AW} \equiv P_A - P_W < 0$, then the generatrix is convex (Figure 3C), while, in the oposite case, $\Delta P_{AW} > 0$, the generatrix is concave (Figure 3D). In both cases the shape of the AW interface can be described by the following equations, which are obtained after double integration of eq 3:[9]

$$z_{AW}(r) = r_{1E}\left[E(\phi_{1E},q_{1E}) - \frac{1}{r r_{1E}}\sqrt{(r^2 - {r_{0E}}^2)({r_{1E}}^2 - r^2)}\right] - r_{0E}\,\mathrm{sgn}(\Delta P_{AW})\,F(\phi_{1E},q_{1E}) + z_{0E} \qquad (r_C < r < r_P) \quad (11)$$

$$\tan\varphi_{AW} = -\mathrm{sgn}(\Delta P_{AW})\frac{k_{1E}(r^2 - {r_{0E}}^2) + r_{0E}}{|k_{1E}|[(r^2 - {r_{0E}}^2)({r_{1E}}^2 - r^2)]^{1/2}} \qquad (r_C < r < r_P) \quad (12)$$

$$k_{1E} \equiv -\mathrm{sgn}(\Delta P_{AW})\Delta P_{AW}/(2\sigma_{AW}) \quad (13)$$

$$r_{1E} \equiv |1/k_{1E} - r_{0E}| \quad (14)$$

$$q_{1E} \equiv (1 - {r_{0E}}^2/{r_{1E}}^2)^{1/2} \quad (15)$$

$$\sin\phi_{1E} \equiv \frac{1}{q_{1E}}(1 - {r_{0E}}^2/r^2)^{1/2} \qquad (r_C < r < r_P) \quad (16)$$

where $F(\phi,q)$ and $E(\phi,q)$ are elliptic integrals of the first and second kind,[10] respectively; r_{0E} and z_{0E} are parameters that should be determined by the boundary conditions at the contact line and at the boundary of the perturbed region (note that $0 < r_{0E} < r_C$, while z_{0E} could be of arbitrary sign).

Oil−Water Interface. It turns out that the oil−water interface may have any of the shapes discussed above (except a planar shape). Depending on the capillary pressure across the OW interface and on the slope angle at the contact line ψ_{OW}, the surface can be spherical or cylindrical or be described by a catenoid, a nodoid, or an unduloid. As shown by Kralchevsky et al.,[9] instead of considering all these cases separately, it is more convenient to distinguish two geometrically different cases: bridge with concave generatrix (Figure 3E) and bridge with convex generatrix (Figure 3F).

The governing parameter which determines the particular shape of the bridge is the product $k_{1B}r_{0B}$, where r_{0B} is the equatorial radius of the OW interface at the plane $z = 0$ and k_{1B} accounts for the pressure jump across the OW interface

$$k_{1B} \equiv \Delta P_{OW}/(2\sigma_{OW}) \quad (17)$$

Note that k_{1B} could have arbitrary sign (positive, negative, or zero). As explained below, the value of r_{0B} is determined in our calculations from the volume of the liquid bridge (which is assumed to be known) and from the thickness of the foam film.

(a) OW Interface with a Neck (Concave OW Interface). The OW interface is concave (Figure 3E) when $k_{1B}r_{0B} \in (-\infty, {}^1/_2)$. In particular, the generatrix of the interface is a nodoid for $k_{1B}r_{0B} \in (-\infty, 0)$, a catenoid for $k_{1B}r_{0B} = 0$, and an unduloid for $k_{1B}r_{0B} \in (0, {}^1/_2)$. The double integration of eq 3 leads to the following expressions for the generatrix of the interface (nodoid or unduloid)[9]

$$z_{OW}(r) = r_{1B}\,\mathrm{sgn}(\Delta P_{OW})\left[E(\phi_{1B},q_{1B}) - \frac{1}{r r_{1B}}\sqrt{(r^2 - {r_{0B}}^2)({r_{1B}}^2 - r^2)}\right] + r_{0B}F(\phi_{1B},q_{1B}) \qquad (k_{1B} \neq 0;\ r_{0B} < r < r_C) \quad (18)$$

$$\tan\varphi_{OW} = \frac{k_{1B}(r^2 - {r_{0B}}^2) + r_{0B}}{|k_{1B}|[(r^2 - {r_{0B}}^2)({r_{1B}}^2 - r^2)]^{1/2}} \qquad (k_{1B} \neq 0;\ r_{0B} < r < r_C) \quad (19)$$

$$r_{1B} \equiv |1/k_{1B} - r_{0B}| \quad (20)$$

$$q_{1B} \equiv (1 - {r_{0B}}^2/{r_{1B}}^2)^{1/2} \quad (21)$$

$$\sin\phi_{1B} \equiv \frac{1}{q_{1B}}(1 - {r_{0B}}^2/r^2)^{1/2} \qquad (r_{0B} < r < r_C) \quad (22)$$

Equations 18 and 19 describe the OW interface in the cases of nodoid and unduloid. If the capillary pressure jump across the OW interface is zero ($k_{1B} = 0$), then the integration of eqs 3 and 4 leads to another result (catenoid)[8,9]

$$z_{OW}(r) = r_{0B}\ln[r/r_{0B} + \sqrt{(r/r_{0B})^2 - 1}] \qquad (k_{1B} = 0;\ r_{0B} < r < r_C) \quad (23)$$

$$\tan\varphi_{OW} = \frac{r_{0B}}{\sqrt{r^2 - {r_{0B}}^2}} \qquad (k_{1B} = 0;\ r_{0B} < r < r_C) \quad (24)$$

The boundary conditions at the equator of the bridge

$$z_{OW}(r_{0B}) = 0;\ \tan \varphi_{OW}(r_{0B}) \rightarrow \infty \qquad (25)$$

have been used to obtain eqs 18, 19, 23, and 24.

(b) OW Interface with a Haunch (Convex OW Interface). The OW interface is convex (Figure 3F) when $k_{1B}r_{0B} \in (^1/_2, +\infty)$. In particular, the generatrix of the interface is an unduloid for $k_{1B}r_{0B} \in (^1/_2, 1)$, a circumference for $k_{1B}r_{0B} = 1$, and a nodoid for $k_{1B}r_{0B} \in (1, +\infty)$. The unduloid and the nodoid can be described by the equations[9]

$$z_{OW}(r) = -(r_{0B} - 1/k_{1B})F(\phi_{2B},q_{2B})r_{1B} + r_{0B}E(\phi_{2B},q_{2B}) \qquad (k_{1B}r_{0B} \neq 1;\ r_C < r < r_{0B}) \quad (26)$$

$$\tan \varphi_{OW} = -\frac{k_{1B}(r^2 - {r_{0B}}^2) + r_{0B}}{|k_{1B}|[(r^2 - {r_{0B}}^2)({r_{1B}}^2 - r^2)]^{1/2}} \qquad (k_{1B}r_{0B} \neq 1;\ r_C < r < r_{0B}) \quad (27)$$

where r_{1B} is given by eq 20 (note that $r_{1B} < r_{0B}$ in this case) and

$$q_{2B} \equiv (1 - {r_{1B}}^2/{r_{0B}}^2)^{1/2} \qquad (28)$$

$$\sin \phi_{2B} \equiv \frac{1}{q_{2B}}(1 - r^2/{r_{0B}}^2)^{1/2} \qquad (r_C < r < r_{0B}) \qquad (29)$$

If the generatrix of the bridge is a circumference of radius $R_S = 2\sigma_{OW}/\Delta P_{OW}$, then it is described by the equation

$$z_{OW}(r) = [(r_{0B} - r)(2R_S + r_{0B} - r)]^{1/2} \qquad (k_{1B}r_{0B} = 1;\ r_C < r < r_{0B}) \quad (30)$$

The particular case of $k_{1B}r_{0B} = {}^1/_2$ corresponds to a cylindrically shaped interface

$$r(z_{OW}) = r_C = \text{const} \qquad (k_{1B}r_{0B} = {}^1/_2) \qquad (31)$$

Matching the Solutions of Laplace Equation for the Different Interfaces. To describe the liquid bridge and the meniscus surrounding it (the perturbed region of the foam film), one should combine the solutions of the Laplace equation of capillarity for the AW, OW, and OA interfaces. This is a nontrivial task, because the particular form of the function describing the OW interface $z_{OW}(r)$ depends on the conditions (three-phase contact angles, film thickness, volume of the bridge); therefore, this function is not known in advance and should be determined in the course of the calculations. Furthermore, a number of parameters in the equations describing the interfaces are also unknown in advance (e.g., the capillary pressures ΔP_{OW}, ΔP_{AW}, and ΔP_{OA}, the radius of the contact line r_C, etc.).

In the following we will assume that the interfacial tensions σ_{AW}, σ_{OW}, and σ_{OA} are prescribed. The three-phase contact angles α_W, α_O, and α_A can be calculated from the relationships[8]

$$\cos \alpha_W = \frac{{\sigma_{OA}}^2 - {\sigma_{OW}}^2 - {\sigma_{AW}}^2}{2\sigma_{OW}\sigma_{AW}} \qquad (32)$$

$$\cos \alpha_O = \frac{{\sigma_{AW}}^2 - {\sigma_{OW}}^2 - {\sigma_{OA}}^2}{2\sigma_{OW}\sigma_{OA}} \qquad (33)$$

$$\cos \alpha_A = \frac{{\sigma_{OW}}^2 - {\sigma_{OA}}^2 - {\sigma_{AW}}^2}{2\sigma_{OA}\sigma_{AW}} \qquad (34)$$

The foam film thickness and the volume of the oil bridge are also assumed to be known.

The configuration of the bridge and the meniscus surrounding it would be completely defined if the three functions $z_{OW}(r)$, $z_{AW}(r)$, and $z_{OA}(r)$ are known—see eqs 8, 11, and 18 (or eq 26 instead of eq 18 if the bridge has a haunch). In these equations we have nine independent parameters that should be defined or determined from the boundary conditions. These are the three capillary pressures (ΔP_{OW}, ΔP_{AW}, and ΔP_{OA}), the radius of the contact line r_C, the vertical displacements z_{0S} and z_{0E}, the parameters of the elliptic functions r_{0E} and r_{0B}, and the radius of the perturbed zone r_P. The other quantities which appear in eqs 8, 11, and 18 (R_{OA}, r_{1E}, k_{1E}, q_{1E}, ϕ_{1E},, r_{1B}, k_{1B}, q_{1B}, ϕ_{1B}) can be calculated from eqs 10, 13−17, and 20−22. A careful analysis of the system shows that we have eight additional equations to determine eight of these nine parameters. These are as follows:

(i) Two equations which match the shape of the perturbed zone with the surrounding foam film, which is considered to be planar and has a given thickness h. These equations express the requirements that the function $z_{AW}(r)$ should be equal to half of the film thickness, while the slope should be zero, at the periphery of the perturbed zone

$$z_{AW}(r = r_P) = h/2 \qquad (35)$$

$$\frac{dz_{AW}}{dr}\Big|_{r=r_P} = 0 \qquad (36)$$

(ii) Two equations which express the requirement that the OW, AW, and OA interfaces should meet each other at the three-phase contact line

$$z_{OW}(r = r_C) = z_{AW}(r = r_C) \qquad (37)$$

$$z_{OW}(r = r_C) = z_{OA}(r = r_C) \qquad (38)$$

(iii) Two equations which stem from the Neumann vectorial triangle at the three-phase contact line

$$\psi_{OA} = \psi_{AW} + \alpha_A - \pi \qquad (39)$$

$$\psi_{OW} = \psi_{OA} + \alpha_O \qquad (40)$$

(iv) One equation expressing the balance of the capillary pressure jumps across the interfaces

$$\Delta P_{OW} = \Delta P_{AW} + \Delta P_{OA} \qquad (41)$$

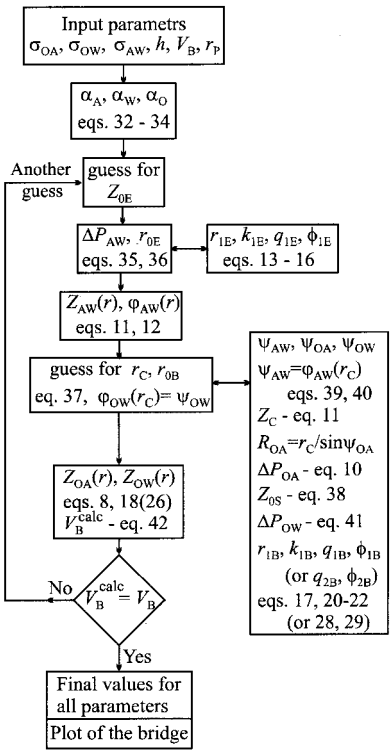

Figure 4. Block scheme of the numerical algorithm used to obtain the equilibrium shape of an oil bridge of a given volume, V_B, in a foam film of deformable surfaces. For simplicity, only the cases when the oil−water interface is generated by a revolution of nodoid or unduloid are presented.

(v) One equation which requires that the volume of the bridge is equal to an initially preset value V_B. The volume of the bridge can be calculated from the equation

$$V_B = 2\pi\int_{r_{0B}}^{r_C} r^2 \tan\varphi_{OW}\, dr + \mathrm{sgn}(\Delta P_{OA})2V_{CAP} \qquad (42)$$

where V_{CAP} is the volume of the spherical "cap" of the bridge confined between the horizontal plane at the three-phase contact line, $z = z_C$, and the OA interface

$$V_{CAP} = \frac{\pi}{6}|H_S|(3r_C^2 + H_S^2);\ H_S = \frac{r_C(1-\cos\psi_{OA})}{\sin\psi_{OA}} \qquad (43)$$

We used eqs 35−42 to determine the values of ΔP_{OW}, ΔP_{AW}, ΔP_{OA}, r_C, z_{0S}, z_{0E}, r_{0E}, and r_{0B}. The radius of the perturbed zone r_P was varied in the calculations as a free parameter. Indeed, we see in the experiment that the radius of the "fish-eye" (the interference pattern from the perturbed zone) increases with time. In reality, the increase of r_P corresponds to the process of drainage of water away from the bridge, caused by the pressure difference between the liquid in the perturbed zone close to the bridge and that in the flat portion of the film (far from the bridge)—see the next section for a more detailed explanation.

The complete algorithm used to "build-up" the bridge on the basis of the above equations is shown in Figure 4.

Numerical Results—Shape and Stability of Oil Bridges

The dependence of the bridge shape on the three-phase contact angles and on the volume of the bridge is examined in this section. The criteria for bridge stability and the regions of stable and unstable bridges are discussed.

Effect of the Three-Phase Contact Angles on the Bridge Shape. Let us consider first how the shape of an equilibrium bridge depends on the three-phase contact angles at a given volume of the bridge. As a reference we will use the volume of an oil drop of diameter equal to the film thickness

$$V_0 = \frac{4\pi}{3}(h/2)^3 \qquad (44)$$

From the viewpoint of the mechanism of antifoam action, liquid bridges of volume V_B on the order of and larger than V_0 are of primary interest.

To give a clear idea about the magnitude of the calculated quantities, we will present the results in dimensional form at given specific values of the interfacial tensions σ_{OA}, σ_{OW}, and σ_{AW} and the film thickness ($h = 2$ μm) comparable to those in our experiments.[1] However, the results can be applied to other values of the interfacial tensions and the film thickness if an appropriate scaling is used. For example, at given values of the interfacial tensions, all geometrical quantities, including the radii of curvature, can be scaled by the film thickness h, while the scaling factor for the capillary pressures is $1/h$.

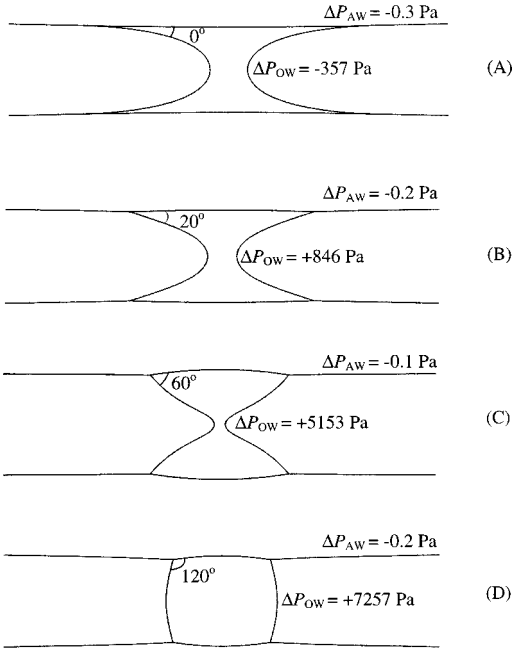

Figure 5. Equilibrium shape of oil bridges at different contact angles water−oil−air: (A) $\alpha_O = 0$; (B) $\alpha_O = 20°$; (C) $\alpha_O = 60°$; (D) $\alpha_O = 120°$. The remaining parameters are $\sigma_{OA} = 20.6$ mN/m, $\sigma_{OW} = 4.7$ mN/m, $h = 2$ μm, $r_p = 100$ μm, and $V_B = V_0 = \pi h^3/6$.

In Figure 5 we plot the reconstructed oil bridges, along with part of the contiguous foam film at (A) $\alpha_O = \theta_{OW} = 0$ and $\alpha_W = 180°$, (B) $\alpha_O = 20°$ and $\theta_{OW} = 16.3°$ and $\alpha_W = 163.7°$, (C) $\alpha_O = 60°$ and $\theta_{OW} = 49.9°$ and $\alpha_W = 130.1°$, and (D) $\alpha_O = 120°$ and $\theta_{OW} = 107.4°$ and $\alpha_W = 72.6°$. The interfacial tensions $\sigma_{OA} = 20.6$ mN/m and $\sigma_{OW} = 4.7$ mN/m were chosen to be the same as those in the experiments described in ref 1. The surface tension of the film σ_{AW} was varied between 25.3 and 18.7 mN/m (see eqs 32−34) in order to scan the range of three-phase contact angles of interest. The volume of the bridge was equal to V_0, while the radius of the perturbed zone in the film r_p was chosen to be equal to 100 μm. Note that the system shown in Figure 5A, $\alpha_O = \theta_{OW} = 0$, corresponds to an oil that is able to spread completely over the film surface (spreading coefficient $S = 0$).

In all these cases we are able to construct bridges which are in mechanical equilibrium with the contiguous meniscus; that is, the capillary pressure balance and the

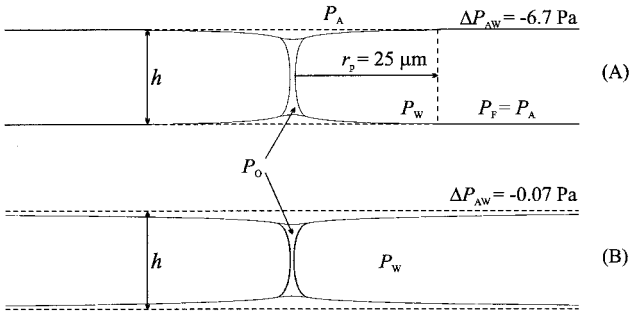

Figure 6. Equilibrium shape of an oil bridge in a foam film at different radii of the perturbed zone: (A) $r_p = 25\ \mu$m; (B) $r_p = 200\ \mu$m. The remaining parameters are $\sigma_{OA} = 20.6$ mN/m, $\sigma_{OW} = 4.7$ mN/m, $\sigma_{AW} = 25.3$ mN/m, $\alpha_O = 0$, $h = 2\ \mu$m, $V_B = V_0 = \pi h^3/6$. The aspect ratio along r and z coordinates is made different from unity to illustrate the shape of the perturbed zone.

three-phase contact angles are satisfied. Note that the bridging coefficients B for the bridges shown in Figure 5A−C are positive—as shown by Garrett,[2] no equilibrium bridges could exist at positive B if the surfaces of the film are assumed to be perfectly planar. This means that equilibrium configurations can be realized only because the surfaces of the foam film are deformable. However, as explained below some of these bridges are in stable equilibrium, while others are in mechanically unstable equilibrium.

The capillary pressures ΔP_{OW} and ΔP_{OA} are typically on the order of $\Delta P_{OW} \approx \Delta P_{OA} \sim 10^2$ to 10^3 Pa (see eq 41). For comparison, the contribution in the Laplace equation of capillarity due to gravity ΔP_G can be estimated to be on the order of $\Delta\rho g h \sim 10^{-2}$ Pa ($\Delta\rho$ is the difference between the mass densities of the phases, and g is the acceleration due to gravity). The latter estimate justifies our approximation to neglect the gravity terms in the overall consideration.

Remarkably, the capillary pressure across the air−water interface ΔP_{AW} is relatively low ($\Delta P_{AW} \sim 0.2-0.3$ Pa) compared to the film−meniscus capillary pressure (~50 Pa), which is the driving force for thinning of the foam film. Therefore, the flux of water away from the bridge, which is created by the curvature of the film surfaces in the perturbed region, should not be very intensive at this value of r_p.

The effect of the increased pressure of the aqueous phase in the perturbed zone on the evolution of the foam film can be understood better by considering how the increase of r_p affects the capillary pressures. In Figure 6 we show the configuration of an oil bridge and indicate the respective capillary pressures at two different radii of the perturbed zone: $r_p = 25\ \mu$m and $r_p = 200\ \mu$m (cf. also with Figure 5A). One sees that the magnitude of the capillary pressure $|\Delta P_{AW}| = (P_W - P_F)$, which indicates how much the pressure in the perturbed film region P_W exceeds the pressure in the planar portion of the film P_F, rapidly decreases with the radius of the perturbed zone (note that $P_F = P_A$, because the nonperturbed portion of the film is planar). This result can be interpreted in the following way. Immediately after the formation of a bridge, the radius of the perturbed zone is relatively small. The corresponding excess pressure in the perturbed zone $P_W - P_F$, is high, and this brings about a flux of water away from the bridge. As a result, the radius of the perturbed zone increases, while the excess of pressure in the perturbed zone decreases with time. When the excess of pressure in the perturbed zone becomes substantially smaller in magnitude than the film−meniscus capillary pressure (which is the driving force for thinning of the whole foam film), then the contribution of the perturbed zone to the overall film thinning becomes negligible. It is important to note that the increase of r_p does not lead to immediate destabilization of the foam film. A perforation of the oil bridge is needed for film rupture.

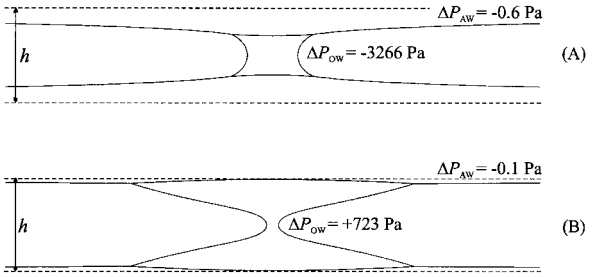

Figure 7. Shape of oil bridges "with neck" of different volume: (A) $V_B/V_0 = 0.3$; (B) $V_B/V_0 = 5$. The remaining parameters are $\sigma_{OA} = 20.6$ mN/m, $\sigma_{OW} = 4.7$ mN/m, $\sigma_{AW} = 25.07$ mN/m, $\alpha_O = 20°$, $h = 2\ \mu$m, and $r_p = 100\ \mu$m.

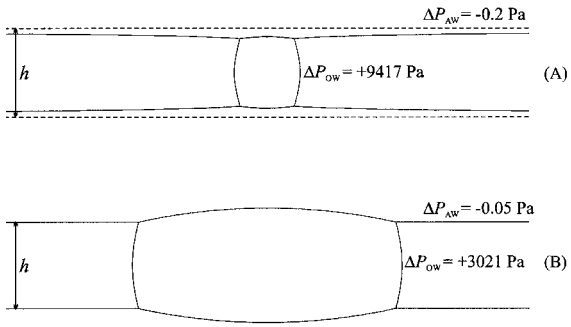

Figure 8. Shape of oil bridges "with haunch" of different volume: (A) $V_B/V_0 = 0.5$; (B) $V_B/V_0 = 15$. The remaining parameters are $\sigma_{OA} = 20.6$ mN/m, $\sigma_{OW} = 4.7$ mN/m, $\sigma_{AW} = 18.7$ mN/m, $\alpha_O = 120°$, $h = 2\ \mu$m, and $r_p = 100\ \mu$m.

Effect of the Oil Volume on the Bridge Shape. The shape of an oil bridge and its stability depend also on its size (see the next subsection for details). For that reason we demonstrate in Figures 7 and 8 how the shape of an oil bridge changes with the increase of the bridge volume with all other parameters fixed (three-phase contact angles, film thickness, and radius of the perturbed zone). The parameters for the bridge shown in Figure 7 are the same as those in Figure 5B ($\theta_{OW} < 0$, positive B), while those for the bridge shown in Figure 8 correspond to those in Figure 5D ($\theta_{OW} > 0$, negative B). For brevity we will adopt the notation from ref 9 and will call "bridges with necks" those of positive B, while those of negative B will be denoted as "bridges with haunch".

The calculations demonstrate that, in general, the capillary pressures across the oil−water and oil−air interfaces change their sign with the increase of the bridge volume for bridges with necks: $\Delta P_{OW} \approx \Delta P_{OA}$ change from negative to positive (see Figure 7). Accordingly, the shape of the bridge also changes: the spherical caps in Figure 7A (negative ΔP_{OA}) are concave, because the pressure in the gas phase is higher than the pressure in the oil, while the caps in Figure 7B (positive ΔP_{OA}) are convex. The oil−water interface in Figure 7A (negative ΔP_{OW}) is generated by revolution of a nodoid, while in Figure 7B (positive ΔP_{OW}) it is generated by revolution of an unduloid. At sufficiently large volume of the bridge, inflection points are observed on the curve describing the oil−water interface, $z_{OW}(r)$—in these points the second derivative of $z_{OW}(r)$ is equal to zero (Figure 7B). As discussed below, the appearance of such inflection points might be an indication for unstable bridges. The capillary pressure

across the air−water interface ΔP_{AW} is always negative and tends to zero with the increase of the bridge volume. However, as pointed out by Garrett,[2,3] perfectly flat film surfaces ($\Delta P_{AW} = 0$) cannot be achieved for such bridges, because the conditions for mechanical equilibrium cannot be satisfied.

Bridges with haunch (negative B) behave in a somewhat different manner—see Figure 8. The capillary pressures ΔP_{OW} and ΔP_{OA} are positive in the whole range of bridge volumes. Correspondingly, the spherical caps of the bridge are convex and no inflection points appear in the function $z_{OW}(r)$, except for very small bridges $V_B/V_0 < 0.2$ at θ_{OW} close to 90°. As discussed below, all these features indicate that the bridges with haunch are stable. It is worth noting that the capillary pressure across the air−water interface ΔP_{AW} changes its sign with the increase of the bridge volume. At sufficiently large bridge volume, ΔP_{AW} becomes positive, which means that the pressure in the perturbed zone is lower than the pressure in the contiguous nonperturbed planar portion of the film ($P_W < P_F$). As a result, such large bridges with haunch will not destabilize the film in any way, because the bridges themselves are stable and, in addition, they do not facilitate the drainage of water from the film.

Stability of Bridges. All of the equilibrium configurations discussed above satisfy the necessary conditions for mechanical equilibrium of the bridge with the contiguous phases. However, not all of these configurations are stable—some of them correspond to local minima in the energy of the system, while others do not.[12,13] The stable bridges will tend to restore their shape if subjected to small mechanical perturbations (e.g., vibrations, local change of the foam film thickness, etc.), because their equilibrium shape corresponds to a local minimum of the energy. On the contrary, the unstable configurations are in mechanical equilibrium, which is vulnerable to any small perturbation of the system, just as in the classical example of a ball placed on the top of a smooth hill. Any small perturbation would displace the unstable bridge from the position of mechanical equilibrium, and will eventually destroy the film. Therefore, our analysis would be incomplete if we do not specify the regions of stable and unstable equilibrium bridges.

Theoretical Approaches to Analyze the Stability of Capillary Systems. The classical approach[11−14] to analyze the stability of capillary systems, such as liquid bridges or pendant drops, consists of formulating an energy functional and subsequent variation of this functional at given, prescribed conditions (e.g., fixed volume of the drop or fixed capillary pressure). The condition for existence of an extremum of this functional (its first variation must be equal to zero) results in formulation of the Laplace equation of capillarity and the Neumann triangle as necessary conditions for mechanical equilibrium. The sign of the second variation of the energy functional indicates whether the respective solution of the Laplace equation corresponds to stable or unstable equilibrium. Although rather rigorous, this approach is very difficult from a mathematical viewpoint and can be applied only to relatively simple capillary systems. Our system (liquid bridge trapped in a fluid film of deformable surfaces) is too complex for such a type of analysis, and other, simpler approaches are preferable.

Substantial progress in the formulation of new criteria for stability has been achieved during the past decade, mainly by scientists working in the fields of applied mathematics and low-gravity physics.[15,16] The conclusions from these studies can be summarized in the following way. The changes in stability of a given capillary system are associated with some particular points in the diagram V_B versus P_C, where V_B is the volume of the liquid bridge and P_C is the capillary pressure jump across the side wall of the bridge ($P_C \equiv \Delta P_{OW}$ in our system). Two types of such particular points have been distinguished in the literature (Figure 9):

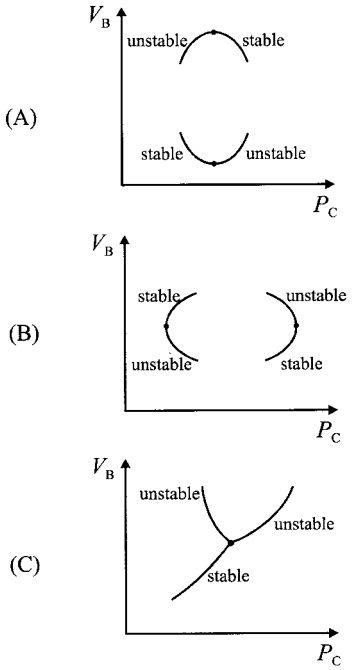

Figure 9. Different types of transition in stability as indicated in the V_B-P_C diagram: (A) limit points which indicate transitions in stability at constant volume of the bridge; (B) limit points indicating transitions in stability at constant capillary pressure; (C) branch points indicating transitions in stability which are associated with changes in the symmetry.

(a) Turning points (termed also fold or limit points), which represent maxima or minima in the curves $V_B(P_C)$, when the perturbation of the equilibrium state is made at fixed volume of the bridge. Alternatively, when the perturbation is made at constant capillary pressure, the turning points represent extrema in the curves $P_C(V_B)$. As pointed out by Lowry and Steen,[16] in reality "the nature of real disturbances lies somewhere between constant pressure and constant volume, and depends on details of the particular apparatus used for observation". Since the support of the bridge in our system is the foam film, which has deformable surfaces, perturbations at variable positions of the three-phase contact lines are possible (z_C and r_C can be varied). Therefore, we may expect that any mode of instability (either at constant pressure or constant volume) will be able to destroy the bridge and the foam film. Note that the sign of the derivative dV_B/dP_C changes at the turning points, which can be used as a convenient way to define them.

(b) Branch points (termed also cusps), where at least three branches of solutions of the Laplace equation of capillarity meet with each other. Vogel[17] has shown that, for a symmetric liquid bridge hanging between two flat

(12) Myshkis, A. D.; Babskii, V. G.; Kopachevskii, N. D.; Slobozhanin, L. A.; Tyuptsov, A. D. *Low Gravity Fluid Mechanics*; Springer-Verlag: New York, 1987.
(13) Eriksson, J. C.; Ljunggren, S. *Langmuir* **1995**, *11*, 2325.
(14) Kralchevsky, P. A. *Langmuir* **1996**, *12*, 5951.
(15) Michael, D. H. *Annu. Rev. Fluid Mech.* **1981**, *13*, 189.
(16) Lowry, B. J.; Steen, P. H. *Proc. R. Soc. London A* **1995**, *449*, 411.
(17) Vogel, T. I. *SIAM J. Appl. Math.* **1989**, *49*, 1009.

parallel plates at a given contact angle and negligible contribution of gravity, the branch point is indicated by the appearance of inflection points in the curve, describing the bridge profile (this is the function $z_{OW}(r)$ in our notation). However, the appearance of inflection points does not always correspond to branch points in the general case.[17]

The above two types of transition points are manifestations of a general principle, formulated first in the theory of bifurcation.[15] According to this principle, a change in the stability of a given system occurs when two (or more) alternative profiles can be realized by a small perturbation, which satisfies the boundary conditions without change of the control parameter (e.g., the prescribed drop volume or capillary pressure).

This short (and somewhat oversimplified) overview of the theoretical approaches in the theory of stability of capillary systems covers only those points which are important for our particular problem. Readers interested in more details are referred to the original articles.[11−17]

Application of the General Approach to the System under Consideration. The application of the approach[15−17] based on identification of turning and branch points is much easier for stability analysis of capillary systems, because one does not need to calculate the second derivative of the energy functional. Instead, one should find the dependence $V_B(P_C)$, starting from small bridges (which are stable in our case) at given three-phase contact angles and film thickness. Any change of the sign of dV_B/dP_C with the increase of the bridge volume would indicate a loss of stability of the bridge at the respective turning point. In parallel, one should examine the minimal bridge volume at which inflection points appear in the curve $z_{OW}(r)$, because these inflection points might also indicate a loss of bridge stability. From all possible curves describing the neck of the bridge, only the unduloid has inflection points,[8,9] which appear at $r = (r_{0B}r_{1B})^{1/2}$. Therefore, the conditions for appearance of inflection points in our system are

$$r_C^2 = r_{0B}r_{1B}; \quad k_{1B}r_{0B} \in (0, {}^1/_2) \tag{45}$$

Equation 45 is equivalent to the requirement that the neck of the bridge is represented by an unduloid whose inflection points coincide with the three-phase contact line. The bridge loses its stability above a critical volume V_B* which meets either of the above two criteria—change of the sign of dV_B/dP_C or appearance of inflection points.

Numerical Results. The above procedure was applied to map the regions of stable and unstable bridges in the plane V_B versus θ_{OW} (by definition $\alpha_W = \pi - \theta_{OW}$)—see Figure 10. The numerical calculations revealed that there are three distinct regions corresponding to three different shapes of the curves $V_B - P_C$ (Figure 10A). In region 1 ($\theta_{OW} < 40°$) the curves V_B versus P_C exhibit two particular points: one point which indicates a change in the sign of the derivative dV_B/dP_C (this point is denoted by M in the graphs) and another point (denoted by I) which indicates the appearance of inflection points on the generatrics of the bridge. Following the general approach described above, one can conclude that the small bridges (those situated on the left from point I) are certainly stable, the larger bridges (those situated above point M) are certainly unstable, and the points between points I and M might be stable or unstable. Additional, much more complex analysis is needed to clarify whether the portion of the V_B-P_C curve confined between points I and M corresponds to stable or unstable bridges—such an analysis requires time and effort (it might require also a further development of the general theory of bridge stability), and we intend to make it in a separate study. It is important to note that the inflection and turning points appear in region 1 at almost the same bridge volume (the relative difference in the bridge volumes corresponding to points I and M is between 10 and 20%), so that the uncertainty for the stability of bridges confined between points I and M has no practical importance from the viewpoint of antifoams.

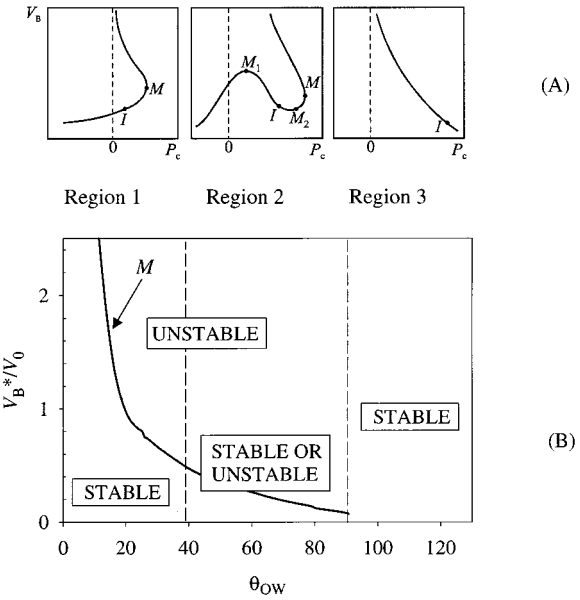

Figure 10. (A) Schematic presentation of the shape of the V_B-P_C curves, which indicate the regions of stable and unstable bridges; points M indicate changes in the sign of the derivative dV_B/dP_C, while points I indicate the appearance of inflection points in the bridge generatrix. (B) Regions of stable and unstable bridges, plotted as functions of the dimensionless bridge volume V_B/V_0 and the angle $\theta_{OW} = (\pi - \alpha_W)$. The remaining parameters are $\sigma_{OA} = 20.6$ mN/m, $\sigma_{OW} = 4.7$ mN/m, $h = 2$ μm, and $r_p = 100$ μm.

The shape of the V_B-P_C curves in region 3, which corresponds to $\theta_{OW} > 90°$ and bridging coefficient $B < 0$, is very simple. The curves V_B versus P_C do not exhibit any point where the derivative dV_B/dP_C changes its sign (V_B is a monotonically decreasing function of P_C). Therefore, one can conclude that the bridges in region 3 are, in general, stable ones. Only for angles θ_{OW} close to 90° and very small bridges ($V_B/V_0 < 0.2$) does one observe the appearance of inflection points on the generatrics of the oil−water interface (i.e., these very small bridges might be unstable).

The shape of the curve V_B versus P_C in region 2 ($40° < \theta_{OW} < 90°$) is more complex. One can distinguish three points (M, M_1, and M_2) where the derivative dV_B/dP_C changes its sign and one point (I) which indicates the appearance of inflection points. Following the general approach (cf. Figure 9), one can deduce that the bridges confined between points M_1 and I are stable, while the bridges situated on the left from point M_1 and on the right from point I (or from point M_2, which is situated nearby) are unstable. Therefore, the large bridges (those of volume above M_1) in region 2 are definitely unstable, while the smaller bridges might be stable or unstable depending on the bridge volume and capillary pressure.

These results are summarized in Figure 10B, where the three regions are separated by vertical dashed lines. The solid curve marked by M indicates the critical volume V_B* which separates the stable bridges (those below the curve) from the unstable ones (above the curve) in region 1. The most important result of the performed analysis

is the discovery of the zone of stable equilibrium bridges in region 1, where the bridging coefficient B is strongly positive. Furthermore, a substantial increase of the critical volume V_B^* is observed at low values of θ_{OW} corresponding to small contact angles α_O, which are usually encountered with silicone antifoams.

We have performed similar calculations at different values of the radius of the perturbed zone, 25 μm $\leq r_P \leq$ 200 μm, which are close to those observed experimentally.[1] The numerical results are very similar, and only slight shifts of the curve shown in Figure 10B (within ca. 20%) are observed—upward for smaller values of r_P and downward for larger values of r_P. From the results of Garrett[2] one may deduce that the region of stability should disappear at $r_P \rightarrow \infty$. However, in real foams the radius of the perturbed zone cannot be larger than the radius of the foam film, which is typically between 100 μm and several millimeters.

It is important to note that the plot in Figure 10B suggests the possibility for a transition of a given bridge from the region of stable bridges into the region of unstable ones. Indeed, the reference volume V_0 will decrease with the film thinning (see eq 44), which will lead to an increase of the ratio V_B/V_0 at fixed actual volume of the bridge. Thus, an initially stable bridge could finally cross the boundary between stable and unstable bridges and rupture the film. To emphasize the role of the variable film thickness, we term the bridges of size below the stability curve in Figure 10 metastable bridges. Another reason to prefer the term "metastable bridge" (instead of "stable bridge") is the existing, though small in magnitude, difference between the pressures in the perturbed zone P_W and those in the flat portion of the film $P_F = P_A$. In fact, our model implies that the bridge is in mechanical equilibrium with the meniscus surrounding it, but the perturbed zone is not in true mechanical equilibrium with the contiguous planar film due to the difference $(P_W - P_F)$. The bridges whose initial relative size (with respect to the film thickness) places them in the region of unstable bridges are termed inherently unstable bridges.

At the end, let us compare briefly the results from the present calculations with the predictions of the simpler model of Garrett.[2,3] According to Garrett's model all bridges with $\theta_{OW} < 90°$ ($B > 0$) could not exist in mechanical equilibrium. The present calculations show that small bridges could be in stable equilibrium at positive values of B (especially at small angles, $\theta_{OW} < 40°$). The large bridges could be in mechanical equilibrium, but this equilibrium is unstable. With respect to the antifoam action, the unstable bridges would destroy the foam films, just as predicted by Garrett's model (although the explanation for the bridge instability is somewhat different). Both models predict stable bridges at $\theta_{OW} > 90°$ ($B < 0$).

Effect of the Prespread Oil Layer on the Bridge Stability

If a thin layer of oil is spread on the surfaces of the foam film, the tension σ_{AW} will be different from that of the film surface in the absence of oil. As a result, the three-phase contact angles and the bridging coefficient will be modified in accordance with eqs 1 and 32−34. Therefore, one can define initial and final bridging coefficients for a given system, just as in the case of the initial and final spreading coefficients.[3]

One intriguing experimental fact, discussed in the Introduction, is the reduced stability of foam films in the presence of a spread oil layer. This observation can hardly

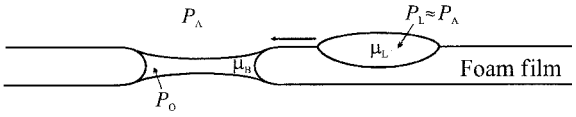

Figure 11. Schematic presentation of the surface transfer of oil from an oil lens, floating on the film surface, toward an oil bridge. The oil transfer is caused by the reduced pressure P_O and hence the reduced chemical potential μ_B of the oil in the bridge. Even if there are no lenses on the film surface, a transfer of oil from a spread oil layer toward the bridge is possible if the chemical potential μ_B is lower than the chemical potential of the oil in the spread layer μ_S.

be explained by differences in the initial and final bridging coefficients, because both of them are strongly positive in the particular experimental system.[1] A much more convincing (and nontrivial) explanation can be deduced from the results shown in Figure 10. Let us assume that an oil bridge is formed from an oil drop (or lens) of volume below the critical one. If the oil is able to spread over the foam film surface, then an exchange of oil between the bridge and the spread layer is possible (see Figure 11). In principle, two opposite directions of oil transfer are possible: (1) spreading of oil from the bridge over the film surfaces or (2) accumulation of oil from the spread layer into the bridge. Which of these two possibilities will be realized in a particular experiment depends on the chemical potentials of the oil in the bridge μ_B and the spread layer μ_S. If the oil phase does not contain solutes, μ_B depends only on temperature and pressure:[18]

$$\mu_B(T,P) = \mu_0(T) + \nu(P_O - P_A) = \mu_0(T) + \nu\Delta P_{OA} \qquad (46)$$

where $\mu_0(T)$ is the chemical potential of a pure bulk oil phase which is under ambient pressure P_A while ν is the molar volume of the oil. Similarly, the chemical potential of the oil in the spread layer μ_S is a function of the layer thickness:[19]

$$\mu_S(T,h) = \mu_0(T) - \nu\Pi_O(h) \qquad (47)$$

Here $\Pi_O(h)$ is the so-called "disjoining pressure" in the spread oil layer. $\Pi_O(h)$ accounts for the intermolecular interactions in the layer and depends in a complex way on the film thickness (for details see refs 9 and 19−23). At large thicknesses $\Pi_O(h \rightarrow \infty) \rightarrow 0$.

If the spread layer is in equilibrium with macroscopic lenses of oil floating on the film surface, then the spread layer will be fully saturated with oil, $\Pi_O(h_{EQ}) \approx 0$ and $\mu_S(T, h) = \mu_0(T)$. In this case, the transfer of oil from and toward the bridge will depend primarily on the capillary pressure ΔP_{OA}. Negative ΔP_{OA} means reduced pressure and chemical potential of the oil in the bridge, which would lead to an influx of oil from the spread layer toward the bridge and vice versa. This influx of oil would increase the actual size of the bridge, and at given parameters, the bridge could cross the boundary separating stable from unstable bridges (see Figure 10B). This is another mechanism (along with the foam film thinning) which could explain the transition from metastable to unstable bridges, which was often observed in the experiments.

It is worthy to note that if the spread layer is not saturated with oil (very thin), then the disjoining pressure Π_O will be positive, and the chemical potential in the layer will be reduced. As a result, the oil from the bridges will spread over the film surfaces. Different possible scenarios

(18) Prigogine, I.; Defay, R. *Chemical Thermodynamics*; Longmans-Green: London, 1954.
(19) Scheludko, A. *Adv. Colloid Interface Sci.* **1967**, *1*, 391.

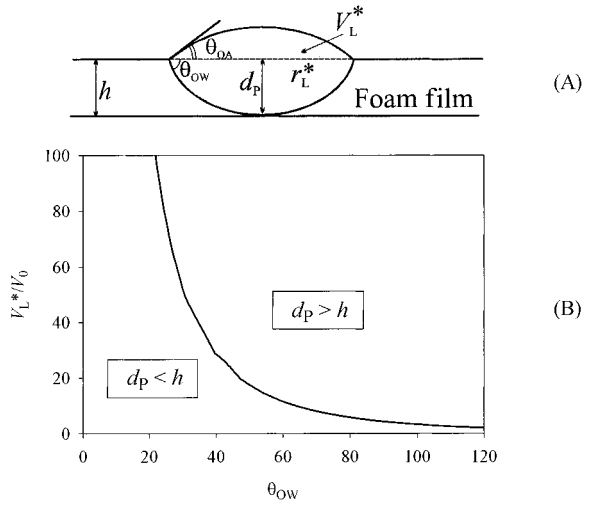

Figure 12. (A) Schematic presentation of an oil lens, whose penetration depth d_p is equal to the foam film thickness h. V_L^* and r_L^* are the volume and radius of the three-phase contact line, respectively, of such a lens. (B) Plot of V_L^*/V_0 as a function of $\theta_{OW} = (\pi - \alpha_W)$; the interfacial tensions in these calculations are $\sigma_{OA} = 20.6$ mN/m and $\sigma_{OW} = 4.7$ mN/m.

could be envisaged in such a case. Our own experiments[1] with one particular system (silicone−silica antifoam in solutions of AOT), however, demonstrated that (1) it was difficult to obtain a bridge in a film without spread oil, because the entry of the antifoam droplets was suppressed, and (2) after the bridge appearance, we observed spreading of oil from the bridge until a final stable configuration was achieved. Most probably, the final stable bridge in these cases was composed of a solid silica framework impregnated with some residual oil. The chemical potential of this residual oil had to be equal to the potential of the spread oil in the nonsaturated layer.

Penetration Depth of Oil Lenses

As shown experimentally in ref 1, oil bridges are often formed from lenses floating on one of the film surfaces. Obviously, a material contact between the bottom of the lens and the opposing film surface is a necessary condition for formation of the bridge in this case[24,25] (Figure 12A). This contact will occur when the film thickness h becomes equal to the so-called "penetration depth" of the lens d_P, which in turn depends on both the three-phase contact angles (α_O, α_W, and α_A) and the volume of oil accumulated in the lens. As far as we know, no quantitative estimate of this effect has been presented till now. For that reason, in the present section we calculate the critical volume of a lens V_L^*, at which the penetration depth becomes equal to the thickness of a foam film and formation of a bridge could be expected. The oil lens is assumed to be deprived of solid silica particles in the following calculations. The effect of silica on the bridge stability and on the penetration depth is discussed later.

It is convenient to present the numerical results in dimensionless form, V_L^*/V_0 as a function of θ_{OW}, because this plot allows one to compare directly the values of V_L^* and V_B^*—see Figure 12B. The calculations are performed at $\sigma_{AO} = 20.6$ mN/m and $\sigma_{OW} = 4.7$ mN/m; σ_{AW} was varied in the range 25.3−18.7 mN/m, which corresponds to a variation of θ_{OW} between 0 and 120°. The values of θ_{OW} and θ_{OA} are calculated from the following equations:[8,24]

$$\cos\theta_{OW} = \frac{\sigma_{AW}^2 + \sigma_{OW}^2 - \sigma_{OA}^2}{2\sigma_{AW}\sigma_{OW}} \tag{48}$$

$$\cos\theta_{OA} = \frac{\sigma_{AW}^2 + \sigma_{OA}^2 - \sigma_{OW}^2}{2\sigma_{AW}\sigma_{OA}} \tag{49}$$

The volume of the critical lens V_L^* is deduced from simple geometrical consideration:

$$V_L^*/V_0 = 2\frac{\sin^3\theta_{OW}}{(1-\cos\theta_{OW})^3}\left[\frac{\sin\theta_{OW}(2+\cos\theta_{OW})}{(1+\cos\theta_{OW})^2} + \frac{\sin\theta_{OA}(2+\cos\theta_{OA})}{(1+\cos\theta_{OA})^2}\right] \tag{50}$$

As seen from Figure 12B, V_L^* is a monotonically decreasing function of θ_{OW}. At small angles an excessively large volume of the critical lens is obtained; in fact, $V_L^* \to \infty$ as $\theta_{OW} \to 0$ (which is equivalent to $\alpha_O \to 0$). This result indicates that the formation of oil bridges would be very difficult at small contact angles of the oil α_O in the absence of silica, because the penetration depth of these lenses is relatively small. This conclusion can be illustrated also with the value of the critical contact radius of the lens r_L^*, at which the penetration depth of the lens becomes equal to the film thickness

$$r_L^*/h = \frac{\sin\theta_{OW}}{(1-\cos\theta_{OW})} \tag{51}$$

The radius of the critical lens tends to infinity ($r_L^*/h \to 2/\theta_{OW} \to \infty$), as $\theta_{OW} \to 0$. Note that the contact angle of silicone oil α_O is usually rather low in solutions of typical surfactants having hydrocarbon tails.

Comparison of the Theoretical Results with Experimental Observations

The aim of this section is to draw the link between the theoretical results and the main experimental observations, which were briefly discussed in the Introduction. The effects of the solid silica particles on the bridge formation and stability are discussed at the end.

First, let us explain how the theoretical model describes the evolution of a metastable bridge, which is formed in a foam film from an oil lens or an emulsified oil drop of diameter close to the film thickness ($V_B \approx V_0$). Immediately after bridge formation, the radius of the perturbed zone is relatively small and the magnitude of the capillary pressure across the air−water interface ΔP_{AW} is relatively large (see Figure 6). This means that the pressure in the perturbed zone is larger than the pressure in the flat portion of the film surrounding the perturbed zone. A radial outflux of water from the perturbed zone should appear as a result of the pressure imbalance. This stage resembles the first stage of the bridging−dewetting mechanism of foam film destruction by hydrophobic solid particles.[3−5] In the bridging−dewetting mechanism, the

(20) Derjaguin, B. V. *Theory of Stability of Colloids and Thin Films*; Plenum Press: New York, 1987; Chapter 1.
(21) Kralchevsky, P. A.; Danov, K. D.; Ivanov, I. B. In *Foams: Theory, Measurements, and Applications*; Prud'homme, K., Khan, S. A., Eds.; Marcel Dekker: New York, 1996.
(22) Hirasaki, G. J. In *Interfacial Phenomena in Petroleum Recovery*; Morrow, N. R., Ed.; Marcel Dekker: New York, 1990; Chapter 2.
(23) Brochard-Wyart, F.; Di Meglio, J. M.; Quere, D., De Gennes, P. G. *Langmuir* **1991**, *7*, 335.
(24) Aveyard, R.; Clint, J. H. *J. Chem. Soc., Faraday Trans.* **1997**, *93*, 1397.
(25) Exerova, D.; Kruglyakov, P. M. *Foam and Foam Films*; Elsevier: Amsterdam, 1997; Chapter 9.

outflux of water from the perturbed zone continues until the three-phase contact lines meet each other on the surface of the antifoam particle (complete dewetting of the particle). On the contrary, the deformability of the oil bridge prevents its complete dewetting in the bridging−stretching mechanism. The oil bridge deforms and acquires a shape which is close to the equilibrium configuration at a given radius of the perturbed zone—this configuration of the bridge and the contiguous perturbed zone appears as "the fish eye" when the foam film is observed in reflected light.[1] The theoretical analysis of the equilibrium shapes of bridges shows that no direct contact of the three-phase contact lines on the surface of the bridge is possible if the bridge is deformable.

The theoretical model predicts that the increase of the radius of the perturbed zone is accompanied by a rapid decrease of the pressure difference between the perturbed zone and the flat portion of the film. Hence, the expansion of the perturbed zone should progressively slow down—this stage corresponds to the metastable bridges observed in ref 1. Since the pressure in the bridge is relatively low ($P_O < P_A \sim P_W$), an accumulation of oil into the bridge from the spread layer should take place until the chemical potential of the oil in the bridge becomes equal to the chemical potential of the spread oil (i.e., $\Delta P_{OW} \approx 0$). The model predicts that, due to the processes of (1) accumulation of oil in the bridge, (2) thinning of the overall foam film, and (3) increase of the radius of the perturbed zone, the relative size of the bridge V_B/V_0 increases with time and approaches the critical boundary, which separates the stable bridges from unstable ones.

Once this critical boundary is reached, any mechanical disturbance (vibrations, hydrodynamic fluxes in the thinning foam film, etc.) would inevitably displace the bridge from its configuration of unstable equilibrium. Any axial contraction of the bridge along the axis of symmetry (due to a local temporal decrease of the foam film thickness in the region of the bridge) would lead to an increase of the equatorial radius of the bridge. As a result, the capillary pressure balance across the oil−water and oil−air interfaces is violated, and a process of spontaneous increase of the equatorial radius of the bridge is induced. This stage in the theoretical model corresponds to the transition from metastable to unstable configuration, as observed in the experiment (ref 1). The bridge expansion would continue until a thin oil layer is formed in the center of the bridge, which eventually ruptures.[1] Alternatively, an axial stretching of the bridge along the axis of symmetry could, in principle, lead to its subdivision into two separate oil lenses attached to the opposing film surfaces without film rupture.

If the bridge is formed from a large drop or lens (as was the case in the experiments with compound A described in ref 1), then its initial size is above the critical volume, $V_B > V_B^*$. Therefore, such a bridge cannot be in stable mechanical equilibrium and it should expand and rupture very fast—this case corresponds to the so-called "inherently unstable" bridges, which were observed to expand and rupture within several milliseconds.[1] The driving force for the process is the lack of balance of the capillary pressures across the oil−water and oil-air interfaces.

We have to emphasize that the experiments in ref 1 were performed with a given system (AOT and silicone-based antifoams) and the above discussion is restricted to that particular system. In other experimental systems the evolution of the oil bridges could be different. For example, if the oil does not spread over the foam film surfaces, an exchange of oil between the bridge and a spread layer cannot occur. As a result, the actual increase of the bridge size due to accumulation of oil from the spread layer is impossible. Then a thinning of the foam film as a whole (which will take more time) will be necessary for overcoming the boundary of the critical bridge volumes V_B^*. One can conclude that the bridges in such systems will take longer to deteriorate and it might take a much longer time for destruction of the foam as a whole.

The consideration so far has been concentrated on the properties of the oil, while the effect of the silica particles has almost been ignored. A rigorous theoretical quantification of the effect of silica on the stability of an oil bridge is practically impossible, because the solid particles break the axial symmetry of the bridge. Indeed, when the thickness of the oil bridge becomes smaller than the dimensions of the solid particles, the latter are expelled toward the periphery of the bridge (where the bridge is thicker), and the axial symmetry is lost. Nevertheless, on the basis of the experimental observations[1] and the theoretical results, we can try to formulate several qualitative hypotheses about the expected impact of solid particles on the bridge formation and stability.

The first hypothesis is that silica substantially facilitates the formation of oil bridges by at least two effects: (1) reduction of the barrier against entry of the oil and (2) increase of the penetration depth of the oil lenses. The first effect was studied in the literature,[3,26] and we will not discuss it in detail here. Our own experiments with a variety of antifoam systems (unpublished results) have demonstrated that oil droplets deprived of solid particles leave the foam films without entering and forming bridges. The foam destruction in these systems occurs through destruction of the Gibbs−Plateau channels, at a much later stage of the foam evolution. The second effect (increase of the penetration depth) is particularly important for small contact angles, $\alpha_O < 10°$, which is the case with silicone oil and with many other antifoams based on hydrocarbons. For instance, it is very difficult to explain how an oil bridge can be formed from a droplet comparable in diameter with the film thickness, without supposing the presence of a solid silica framework inside the drop. Indeed, the entry of the drop on one of the film surfaces would lead to fast formation of a very flat lens, and the contact with the opposing film surface would require a very long time until a further thinning of the foam film reduces its thickness to become comparable with the penetration depth of the lens. On the contrary, the presence of a solid silica framework would preserve the dimensions of the drop even after the first contact with one of the film surfaces, and a second entry (and bridge formation) becomes possible soon after the first one. Therefore, one can conclude that the rupture of the foam films observed in our experiments is closely related to the presence of silica in the used antifoam formulations.

On the other hand, one may expect that the presence of silica in the oil bridges will stabilize them. The main reason for this stabilizing effect is the fact that part of the oil fills up the space in the solid silica framework. The silica framework plays the role of a nondeformable reservoir of oil, which does not participate in the stretching of the bridge. Thus, an excess of oil (over the volume calculated in the section Numerical Results) is needed for formation of unstable bridges. A rough estimate of the nonactive oil, which is "arrested" by the silica framework, can be deduced from the composition of the silica−oil aggregates observed in exhausted antifoams. As shown

(26) Bergeron, V.; Cooper, P.; Fischer, C.; Giermanska-Kahn, J.; Langevin, D.; Pouchelon, A. *Colloids Surf., A: Physicochem. Eng. Aspects* **1997**, *122*, 103.

by Pouchelon and Araud,[27] the exhausted, inactive aggregates contained about 17 wt % silica and 83 wt % silicone oil. Therefore, about four parts of silicone are firmly associated with each part of silica and do not participate in the foam destruction process.

Conclusions

The present study has been inspired by the experimental results described in ref 1. A further development of the model by Garrett[2,3] about the stability of oil bridges in liquid films has been necessary to explain the main experimental observations. The main new features of the theoretical model described in the present paper are the following:

The deformability of the foam film surfaces, which was observed in the experiment, has been explicitly taken into account. This modification makes the model much more complex, and a variety of possible configurations of the bridge and the meniscus surrounding it has to be considered (Figures 5-8).

The theoretical results show that oil bridges might be in equilibrium with the meniscus surrounding them even if the bridging coefficient B is positive. This equilibrium is achieved at the expense of some difference between the pressure in the perturbed zone of the foam film (close to the bridge) and the pressure in the planar portion of the film, far away from the bridge—see Figure 6. In principle, this pressure difference brings about an outflux of water from the perturbed region (similarly to the process of dewetting of solid particles in the well-known bridging−dewetting mechanism), but its magnitude sharply decreases with the radius of the perturbed zone. As a result, after some expansion of the perturbed region, the outflux of water becomes so slow that it can be neglected in the time scale of the film-thinning process. The expansion of the perturbed zone does not lead to a complete dewetting of the bridge (as is the case with nondeformable hydrophobic particles).

The equilibrium configuration of the bridge and the contiguous meniscus could be either stable or unstable, depending on the relative size of the bridge as compared to the film thickness. At positive B the small bridges might be in stable or unstable equilibrium, while the large bridges are always in an unstable equilibrium (see Figure 10). The critical volume separating stable from unstable bridges depends on the three-phase contact angles (i.e. on the value of B). Once shifted from their equilibrium state, the unstable bridges spontaneously expand (due to lack of balance of the capillary pressure jumps at oil−air and oil−water interfaces) and eventually rupture the foam film. At negative values of B, the bridges are in stable equilibrium with the contiguous meniscus, just as predicted by Garrett.[2,3]

The observed strong impact of the spread oil layer on the bridge stability[1] is explained by an actual increase of the bridge volume with time. In this way an initially small, stable bridge could cross the boundary between stable and unstable bridges. The process is governed by the difference in the chemical potentials of the oil in the bridge and in the spread layer (Figure 11).

The penetration depth of oil lenses (deprived of silica particles) is calculated and compared with the thickness of the foam film (Figure 12). It is shown that for small contact angles α_O which are often encountered in practice, the penetration depth is so small that the formation of bridges in the absence of silica would be very difficult. Therefore, one of the roles of silica in mixed solid−liquid antifoams is to increase the penetration depth of the lenses. On the other hand, the silica can stabilize to some extent the oil bridges, and an excess of oil is necessary for formation of unstable bridges in the presence of silica.

The obtained theoretical results are not restricted to the experimental system studied in ref 1. All of the above conclusions can be transferred with minor modifications to any antifoam−surfactant couple, when oil-based antifoams are considered. However, one has to bear in mind that the real systems are so rich in phenomena[28] that other effects (e.g., the kinetics of adsorption of surfactant on the interfaces) could also be important in other particular systems and have to be taken into account. The consistent comparison of our experimental results[1] with the theoretical predictions gives us the confidence that we cover the most important phenomena and processes in our experimental system. New experimental studies with different systems are currently under way, which will hopefully clarify the generality of the ideas presented in this article.

Acknowledgment. The author is indebted to Dr. P. Cooper (Rhodia Silicones), Professor P. Kralchevsky (University of Sofia), and Dr. K. Danov (University of Sofia) for useful discussions. The help of Mr. N. Marekov, who performed some of the numerical calculations, and Mrs. Paraskova (University of Sofia), who prepared some of the figures, is gratefully acknowledged.

LA990214Y

(27) Pouchelon, A.; Araud, A. *J. Dispersion Sci. Technol.* **1993**, *14*, 447.

(28) *Defoaming: Theory and Industrial Applications*; Garrett, P. R., Ed.; Marcel Dekker: New York, 1993; Chapters 2−8.